VIP Catalyst Optimization

DOI: 10.1002/anie.200907247

^{1}H DOSY Spectra of Ligands for Highly Enantioselective Reactions—A Fast and Simple NMR Method to Optimize Catalytic Reaction Conditions**

*Katrin Schober, Evelyn Hartmann, Hongxia Zhang, and Ruth M. Gschwind**

The demand for enantiopure chemicals, for example, natural products, pharmaceuticals, or materials, has been increasing rapidly for years, and the global market is continually expanding.[1] In the field of asymmetric catalysis, transition-metal catalysts using chiral ligands represent one of the most effective and versatile approaches.[2] However, the development of highly efficient catalysts is often an unpredictable, challenging, and time-consuming process. Accordingly, every method that shortens this laborious procedure or allows an assessment of selectivity contributions is highly valued. In this context, rational models were developed to predict asymmetry in resulting products, for example, Cram's rule and the Felkin–Anh model,[3] and quadrant models.[4,5] Furthermore, combinatorial libraries provide empirical strategies for ligand selection.[6–8] With regard to temperature optimization, the isoinversion principle provides a general model for reactions with two or more selectivity steps.[9] At present, the rational models have to address more complex issues because of the importance of noncovalent interligand interactions in organometallic complexes.[10] Even weak π–π interactions were found to influence complex structures,[11,12] for example, a *cis* coordination of the ligands was found for a bis(phosphonite) Pt complex and a bis(phosphoramidite) Pd complex; this coordination was explained by weak intermolecular interactions.[13,14]

In a recent study, we reported a temperature-dependent interconversion, which was potentially caused by interligand interactions, of various phosphoramidite copper complexes.[15] This result raised the question of whether there is a fast and easy way to predict ligand-driven changes of the active catalysts, either by interconversion or by aggregation phenomena. However, to the best of our knowledge, no simple and general procedure has been presented to date that reliably predicts temperature-dependent changes of transition-metal catalyst sizes. Such a prediction would allow a fast determination of the temperature range applicable to the desired catalytic reaction.

Herein, we present the first aggregation study of selected phosphoramidite ligands and their transition-metal complexes. The aggregation trends of the ligands, the complexes of which can catalyze highly enantioselective reactions, reveal that an easy and fast DOSY screening of the free ligands allows a prediction of the aggregation trends of their transition-metal complexes, even without knowledge about their structures. In addition, the applicability limits of this method are discussed and the type of interligand interactions is addressed.

Chiral phosphoramidites have emerged as one of the privileged ligand structures, with increasing applications in various asymmetric catalytic reactions with excellent enantioselectivies.[16–23] Therefore, **1** and **2** (Scheme 1), which show high selectivities in catalysis, were chosen as model systems that represent the well-known binaphthol- and biphenol-based ligand families.[24,25] In addition, the ligand **3**, which shows a lower selectivity, was used to investigate the influence of reduced bulkiness and lack of rotational processes on the aggregation trends. The effects of different transition metals, complex stoichiometries, and geometries were investigated on the complexes [{CuLX}$_3$], [CuL$_3$X], [{CuLX}$_2$], [PdL$_2$Cl$_2$], [Pd**3**$_4$Cl$_2$], and [Ir(cod)LCl] (Scheme 1).

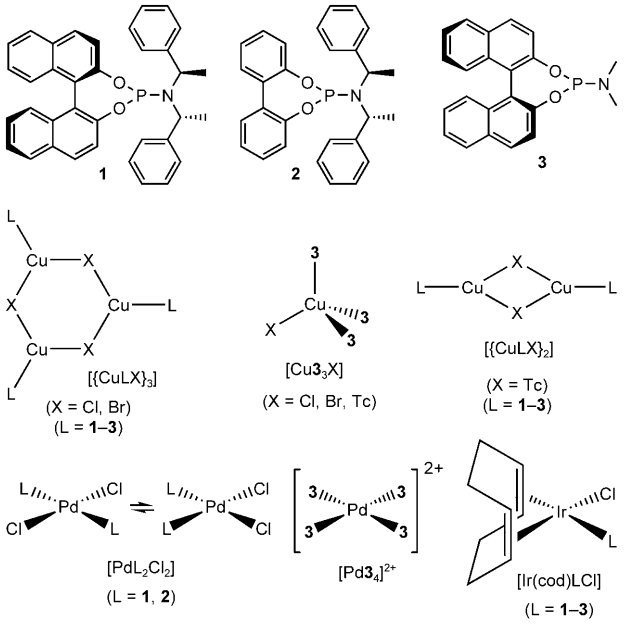

Scheme 1. Phosphoramidite ligands and transition-metal complexes investigated in terms of aggregation trends (Tc = 2-thiophene-carboxylate; cod = 1,5-cyclooctadiene).

[*] K. Schober, E. Hartmann, Dr. H. Zhang,[+] Prof. Dr. R. M. Gschwind
Institut für Organische Chemie, Universität Regensburg
Universitätsstraße 31, 93053 Regensburg (Germany)
Fax: (+49) 941-943-4617
E-mail: ruth.gschwind@chemie.uni-regensburg.de

[+] Current address:
Institute of Applied Chemistry, Shanxi University (China)

[**] This work was supported by the DFG GS13/1-1.

Supporting information for this article is available on the WWW under http://dx.doi.org/10.1002/anie.200907247.

Firstly, temperature-dependent ^{1}H DOSY NMR spectra of the free ligands were measured, and viscosity- and temperature-corrected diffusion coefficients were calculated to gain an insight into the aggregation between the pure ligands. The resulting normalized aggregation curves are presented in Figure 1 a. All three phosphoramidite ligands are monomeric at 270 K and form aggregates below a certain temperature threshold with averaged aggregation numbers up to 2. The individual progression of the aggregation curves differ from each other with respect to the threshold temperatures and the subsequent slopes. The smallest ligand **3** shows the highest temperature threshold of 230 K but the lowest slope. In contrast, ligands **1** and **2**, which afford high enantioselectivities, are both sterically more demanding, have more rotational degrees of freedom, and do not aggregate until 210 K. Below this temperature, both ligands show pronounced aggregation trends, with **2** reaching higher aggregation numbers than **1**.

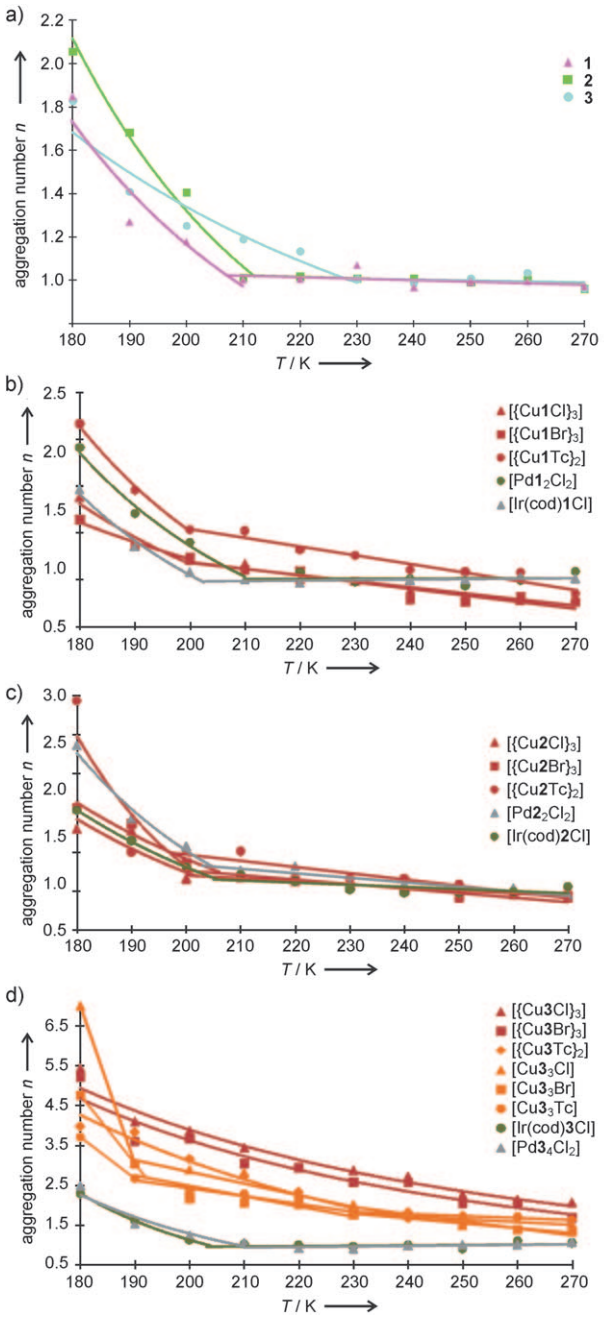

Figure 1. Temperature-dependent aggregation of a) free ligands **1**–**3** and b–d) their complexes in CD_2Cl_2 (0.02 M), based on η/T-corrected diffusion coefficients. η = viscosity.

The aggregation trends of the transition-metal complexes of **1** and **2** were subsequently investigated (Figure 1 b, c). Stable chemical shifts and intensity distributions in the corresponding ^{31}P NMR spectra exclude temperature-dependent interconversion of different complexes species, as previously shown for $[Cu_2L_3X_2]$ complexes (L = **2**, X = I).[15] Thus, all the presented curves result from aggregation of the complexes.[26] All complexes are essentially monomeric at temperatures above 210 K. Between 210 K and 200 K, kinks are observed in all aggregation curves, and complexes with **2** show slightly higher aggregation numbers at low temperatures than those with **1**. A comparison of the data in Figure 1 a–c shows that the aggregation behavior of the transition-metal complexes closely reflects the aggregation trend of the corresponding free ligands. Only the aggregation starting point shifts by up to 10 K to lower temperatures and slight aggregation of some complexes occur above 210 K. This close similarity indicates that the aggregation behavior of complexes with **1** and **2** is dominated by the ligand properties. Variations in the transition metal and the complex geometry, and even the presence of additional ligands with comparably low aggregation tendencies (such as cod) have only marginal effects.

For complexes with ligands such as **1** and **2**, ligand-dominated aggregation might be plausible because of the effective steric shielding from the ligands. However, for considerably smaller ligands with reduced aggregation trends, other phenomena may also contribute to the changes in the complex volume that occur with decreasing temperature. Therefore, the limits of applicability for the transfer of aggregation trends from free ligands to their transition-metal complexes were tested on **3**. Previous synthetic and structural studies of **3** showed that its reduced bulkiness allows crystallization of otherwise inaccessible complexes,[27] favors the formation of complexes with higher ligand/transition metal ratios,[28] and provides only moderate *ee* values compared to **1** and **2**.[25] Consistent with these features of **3**, aggregation curves similar to those of the free ligand with a kink at 230 K were observed (Figure 1 d), as well as aggregation curves with higher aggregation numbers arising from oligomerization (orange), with a continuous aggregation indicating a salt-mediated polymerization (dark red), and with low-temperature shifts of the kink (green and gray). These results hint at entropic contributions or intracomplex saturation (for details see the Supporting Information). The presented data show that the aggregation trends of all investigated transition-metal complexes with the highly stereoselective ligands follow nearly exactly the aggregation of the free ligands, whereas such an aggregation prediction is limited for small and moderately selective ligands that are not suitable for asymmetric catalysis.

We recently described the interconversion of an active catalytic species $[Cu_2L_3X_2]$ into $[Cu_2L_4X_2]$ (L = **2**, X = I), which resulted in reduced *ee* values.[15] Interestingly, the reported temperature threshold of this interconversion is in agreement with the aggregation kinks described in Figure 1 a,c, thus suggesting similar interligand interactions for intra- and intermolecular processes, and opening up a new screening possibility at a very early stage of the catalyst development. An easy and fast DOSY screening of the aggregation properties of sterically demanding ligands that afford high enantioselectivities allows a prediction of the aggregation trends of their transition-metal complexes.

In addition, the mechanism behind the described aggregation phenomena was addressed. Titration studies of **1** and **2** with chlorobenzene showed gradual disaggregation of both ligands.[29–31] This phenomenon suggests that π–π interactions between the ligands play an important role in the aggregation process. Thus, the contributions of the biphenyl or binaphthyl moiety to the π–π interactions were analyzed and compared to those of the phenyl rings on the N substituent. A comparison of the aggregation trends of **1**–**3** (Figure 1 a) showed that the lack of the phenyl groups on the amine moiety of **3** results in a minor slope because only the binaphthyl group contributes to π–π interactions. In addition, **3** achieves significantly lower aggregation numbers than **2** at 180 K, thus indicating that one biphenyl and two phenyl groups can form more favorable π–π interactions at low temperatures than the rigid binaphthyl group, despite similar aromatic sizes. Furthermore, the larger aggregation slopes of **1** and **2** in combination with the low-temperature shift of the aggregation threshold suggest that rotational processes of, or within, the $N[CH(CH_3)Ph]_2$ group have to slow down before the phenyl groups can contribute significantly to the aggregation. In this context, the rate constants of the rotational movements that affect the phenyl ring can be used to estimate the involvement of the phenyl groups in π–π or CH–π interactions.[32] For this purpose, rotations around the N–C bond were investigated because two separate methine signals were detected at 180 K; these signals can be used to analyze the rotational process by dynamic NMR through spectra simulation and Eyring plots (see Figure 2 and the Supporting Information).

The Eyring plots of **1** and **2** (Figure 3) show two straight lines with pronounced kinks at 220 K and 230 K, respectively (gray bars), thus indicating the presence of two different mechanisms that are dominant at high and low temperatures. In the high-temperature region, small $\Delta H^{\neq}$ values in combination with large negative $\Delta S^{\neq}$ values indicate crowded transition states, which are typical for inversion processes on nitrogen atoms (for details see the Supporting Information).[33–36] At low temperatures, the thermodynamic parameters reveal that only the rotational process remains (for details see the Supporting Information). The corresponding rate constants (see table in Figure 3) show that the rotational process in **2** nearly stops at low temperatures, whereas the rate constants of **1** are significantly higher. This result shows that the π–π or CH–π interactions between the phenyl groups and the biphenyl moiety in **2** are essentially stronger than those between the phenyl groups and the binaphthyl moiety in **1**. In addition, the lower rotational movements in **2** seem to support the intermolecular interactions, as reflected in the slightly higher aggregation slope of **2**. Furthermore, the strong interaction between the phenyl groups and the biphenyl backbone in **2** corroborates the hypothesis of induced atropisomerism, which was used to explain the high enantioselectivities afforded by this ligand[25] and was recently reported for rhodium complexes.[37]

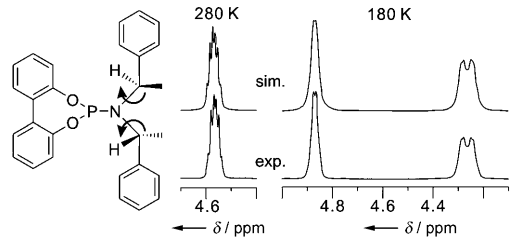

Figure 2. Methine sections from the experimental and simulated ^{1}H NMR spectra of ligand **2** at 280 K and 180 K.

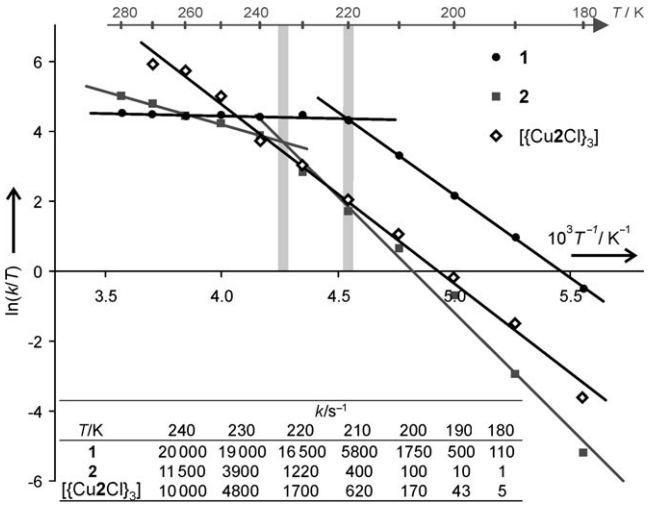

k/s⁻¹ T/K	240	230	220	210	200	190	180
1	20000	19000	16500	5800	1750	500	110
2	11500	3900	1220	400	100	10	1
[{Cu**2**Cl}$_3$]	10000	4800	1700	620	170	43	5

Figure 3. Eyring plots of free ligands **1** and **2** as well as complex [{Cu**2**Cl}$_3$]. The table shows the corresponding rate constants *k* based on simulated ^{1}H NMR spectra.

In contrast to the free ligand **2**, no inversion occurred and only rotational processes were detected for the complex [{Cu**2**Cl}$_3$]. These results are in agreement with slightly reduced P–N bond lengths found in crystal structures,[27] and which might also be caused by the more crowded transition state of the inversion. However, a comparison of the rotational processes in **2** and [{Cu**2**Cl}$_3$] shows rate constants of the same order of magnitude for both systems, thus implying that the rotational degrees of freedom of the N substituents in **2** are not considerably affected upon complexation. This result may explain the similarity of the aggregation trends of **2** and [{Cu**2**Cl}$_3$] and moreover may give a hint at the general structural properties of so-called priviliged ligands that can be used with several transition metals and in various reactions.

In summary, the first self-aggregation studies of phosphoramidites and their transition-metal complexes are reported, and insights into the aggregation mechanism are

presented. For complexes with large ligands, the aggregation of the transition-metal complexes directly follows the aggregation behavior of the corresponding free ligands. In contrast, for complexes with small ligands, phenomena other than ligand-dominated aggregation can occur. Disaggregation studies, the interpretation of the aggregation curves, and dynamic NMR analyses of the internal dynamic within the ligands revealed that rotational processes define the starting temperature of aggregation and allow insights into the different contributions of the aromatic systems to aggregation. Interestingly, complexation only marginally affects the rotational processes within the ligands. This observation may explain the similar aggregation trends observed and the success of phosphoramidite ligands as privileged ligands in a broad range of transition-metal catalysts.

These results now open up a new screening possibility for a faster temperature optimization in the development of transition-metal catalysts. For sterically demanding phosphoramidite ligands, which are suited for asymmetric catalysis, an easy and fast DOSY screening of the free ligand allows a reliable prediction of the temperature-dependent aggregation behavior of its transition-metal complexes. Even the contribution of different transition metals, complex stoichiometries, complex geometries, and additional ligands with low aggregation tendencies do not affect the predictability of aggregation. The independence of this method from the structural knowledge of the catalytically active species makes this screening method very valuable for catalyst optimization, even in the early development stage. The presented method for aggregation screening by DOSY measurements may be expanded to other ligand families and can be used for solvent optimization in terms of solvent-dependent aggregation phenomena. For any desired catalytic system, two DOSY screenings, one of the free ligand and one of the complex, can be used to validate the applicability of this method. Further work is planned to corroborate this hypothesis.

Received: December 23, 2009

Keywords: aggregation · asymmetric catalysis · catalyst optimization · NMR spectroscopy · N, P ligands

[1] *Asymmetric Catalysis on Industrial Scale: Challenges, Approaches and Solutions*, Wiley-VCH, Weinheim, **2004**.
[2] V. Caprio, J. Williams, *Catalysis in Asymmetric Synthesis*, 2nd ed., Wiley, New York, **2009**.
[3] A. Mengel, O. Reiser, *Chem. Rev.* **1999**, *99*, 1191 – 1224.
[4] J. K. Whitesell, *Chem. Rev.* **1989**, *89*, 1581 – 1590.
[5] P. Walsh, M. Kowzlowski, *Fundamentals Of Asymmetric Catalysis*, University Science Books, **2008**.
[6] M. T. Reetz, *Angew. Chem.* **2002**, *114*, 1391 – 1394; *Angew. Chem. Int. Ed.* **2002**, *41*, 1335 – 1338.
[7] C. Gennari, U. Piarulli, *Chem. Rev.* **2003**, *103*, 3071 – 3100.
[8] K. Ding, *Chem. Commun.* **2008**, 909 – 921.
[9] H. Buschmann, H.-D. Scharf, N. Hoffmann, P. Esser, *Angew. Chem.* **1991**, *103*, 480 – 518; *Angew. Chem. Int. Ed.* **1991**, *30*, 477 – 515.
[10] B. Breit, *Angew. Chem.* **2005**, *117*, 6976 – 6986; *Angew. Chem. Int. Ed.* **2005**, *44*, 6816 – 6825.
[11] E. A. Meyer, R. K. Castellano, F. Diederich, *Angew. Chem.* **2003**, *115*, 1244 – 1287; *Angew. Chem. Int. Ed.* **2003**, *42*, 1210 – 1250.
[12] P. Dotta, A. Magistrato, U. Rothlisberger, P. S. Pregosin, A. Albinati, *Organometallics* **2002**, *21*, 3033 – 3041.
[13] A. Gillon, K. Heslop, D. J. Hyett, A. Martorell, A. G. Orpen, P. G. Pringle, C. Claver, E. Fernandez, *Chem. Commun.* **2000**, 961 – 962.
[14] S. Filipuzzi, P. S. Pregosin, A. Albinati, S. Rizzato, *Organometallics* **2006**, *25*, 5955 – 5964.
[15] K. Schober, H. Zhang, R. M. Gschwind, *J. Am. Chem. Soc.* **2008**, *130*, 12310 – 12317.
[16] B. L. Feringa, *Acc. Chem. Res.* **2000**, *33*, 346 – 353.
[17] A. Alexakis, C. Benhaim, *Eur. J. Org. Chem.* **2002**, 3221 – 3236.
[18] A. Alexakis, J. E. Bäckvall, N. Krause, O. Pàmies, M. Diéguez, *Chem. Rev.* **2008**, *108*, 2796 – 2823.
[19] S. R. Harutyunyan, T. den Hartog, K. Geurts, A. J. Minnaard, B. L. Feringa, *Chem. Rev.* **2008**, *108*, 2824 – 2852.
[20] A. J. Minnaard, B. L. Feringa, L. Lefort, J. G. de Vries, *Acc. Chem. Res.* **2007**, *40*, 1267 – 1277.
[21] Z. Hua, V. C. Vassar, H. Choi, I. Ojima, *Proc. Natl. Acad. Sci. USA* **2004**, *101*, 5411 – 5416.
[22] R. K. Thalji, J. A. Ellman, R. G. Bergman, *J. Am. Chem. Soc.* **2004**, *126*, 7192 – 7193.
[23] I. S. Mikhel, G. Bernardinelli, A. Alexakis, *Inorg. Chim. Acta* **2006**, *359*, 1826 – 1836.
[24] A. Alexakis, S. Rosset, J. Allamand, S. March, F. Guillen, C. Benhaim, *Synlett* **2001**, 1375 – 1378.
[25] L. A. Arnold, R. Imbos, A. Mandoli, A. H. M. de Vries, R. Naasz, B. L. Feringa, *Tetrahedron* **2000**, *56*, 2865 – 2878.
[26] Use of the aggregated complex leads to lower conversion than the monomer in the copper-catalyzed conjugate addition with [{Cu**3**Tc}$_2$].
[27] A. H. M. de Vries, A. Meetsma, B. L. Feringa, *Angew. Chem.* **1996**, *108*, 2526 – 2528; *Angew. Chem. Int. Ed.* **1996**, *35*, 2374 – 2376.
[28] H. Zhang, R. M. Gschwind, *Chem. Eur. J.* **2007**, *13*, 6691 – 6700.
[29] Chlorobenzene is ideal for this purpose because it matches the dielectric constant of the solvent CH_2Cl_2 and thus avoids compound-driven change of aggregation.
[30] G. Bellachioma, G. Ciancaleoni, C. Zuccaccia, D. Zuccaccia, A. Macchioni, *Coord. Chem. Rev.* **2008**, *252*, 2224 – 2238.
[31] D. Zuccaccia, G. Bellachioma, G. Cardaci, C. Zuccaccia, A. Macchioni, *Dalton Trans.* **2006**, 1963 – 1971.
[32] This close connection between interaction strength and reduction of dynamic processes is well known in molecular recognition processes and was also observed in NMR investigations of charge-assisted hydrogen-bond networks, see: a) D. H. Williams, E. Stephens, D. P. O'Brien, M. Zhou, *Angew. Chem.* **2004**, *116*, 6760 – 6782; *Angew. Chem. Int. Ed.* **2004**, *43*, 6596 – 6616; b) P. Ghosh, G. Federwisch, M. Kogej, C. A. Schalley, D. Haase, W. Saak, A. Lutzen, R. M. Gschwind, *Org. Biomol. Chem.* **2005**, *3*, 2691 – 2700; c) G. Federwisch, R. Kleinmaier, D. Drettwan, R. M. Gschwind, *J. Am. Chem. Soc.* **2008**, *130*, 16846 – 16847.
[33] M. I. Rodríguez-Franco, I. Dorronsoro, A. Castro, A. Martínez, *Tetrahedron* **2000**, *56*, 1739 – 1743.
[34] C. H. Bushweller, J. W. O'Neil, H. S. Bilofsky, *Tetrahedron* **1971**, *27*, 5761 – 5766.
[35] C. H. Hackett Bushweller, C. Y. Wang, J. Reny, M. Z. Lourandos, *J. Am. Chem. Soc.* **1977**, *99*, 3938 – 3941.
[36] M. J. S. Dewar, W. B. Jennings, *Tetrahedron Lett.* **1970**, *11*, 339 – 342.
[37] C. Monti, C. Gennari, U. Piarulli, *Chem. Eur. J.* **2007**, *13*, 1547 – 1558.

